# A novel method for moving vehicle tracking based on horizontal edge identification and local autocorrelation images

## Un nuevo método para el seguimiento de un vehículo en movimiento mediante identificación de borde horizontal y autocorrelación local de imágenes

**Hongjin Zhu[1], Honghui Fan[1], Feiyue Ye[1,2], Shisong Zhu[3] and Pengzhen Gan[4]**

[1] School of Computer Engineer, Jiangsu University of Technology, Zhongwu Road 1801#, Changzhou, 213001, Jiangsu, China
[2] Key Laboratory of Cloud Computing and Intelligent Information Processing of Changzhou City, Zhongwu Road 1801#, Changzhou, 213001, Jiangsu, China
[3] School of Computer Science and Technology, Henan Polytechnic University, Shiji Road 2001#, Jiaozuo, 454000, Henan, China
[4] Department of Technology Development, Management System Integrator, Matsue Road 1-5-7#, Yamagata, 990-2473, Yamagata, Japan.

**DOI: http://dx.doi.org/10.6036/7844** | Recibido: 14/10/2015 • Aceptado: 25/11/2015

## RESUMEN

• Se propone un novedoso método para el seguimiento de vehículos en movimiento basado en la identificación por autocorrelación local (LAC) y en el perfil horizontal (HE) con objeto de mejorar su identificación. Las imágenes de autocorrelación local se generaron como pre-tratamiento para la identificación de perfil horizontal, de forma que las características de dicho perfil horizontal pudieran ser reforzadas en caso de verse reducidas por la influencia de las condiciones climáticas. Un modelo de antecedentes robusto basado en el método de olvido exponencial (EFM) puede ser obtenido, detectando las zonas del vehículo en movimiento a través de la eliminación de antecedentes. Se detectó el perfil horizontal estable del vehiculo a través del seguimiento del mismo, la cual fue normalizada posteriormente en la secuencia de imágenes para mejorar la tasa de detección. Se utilizó la distancia de la coordenada del baricentro de los perfiles horizontales para seguir los vehículos en las secuencias de vídeos de tráfico. Las coordenadas del baricentro se modificaron utilizando un coeficiente de corrección para asegurar el efecto de la etapa de seguimiento. Las zonas donde se localizan el vehículo se marcaron utilizando cajas rectangulares en los fotogramas durante la etapa de seguimiento del vehículo. Se emplearon vídeos de tráfico en diferentes condiciones complejas (tiempo neblinoso, fuerte luz solar, mañana y tarde) así como imágenes de prueba para verificar la eficacia del método propuesto. Los resultados experimentales muestran que una mayor tasa de identificación de vehículos en movimiento es obtenido a través del método propuesto. El novedoso método propuesto puede usarse para mejorar los resultados de los sistemas inteligentes de transporte.

• **Palabras clave:** Seguimiento de vehículos, Autocorrelación local, Perfiles horizontales, Método de olvido exponencial.

## ABSTRACT

A novel method for moving vehicle tracking was proposed to improve the vehicle identification rate on the basis of local autocorrelation (LAC) and horizontal edge (HE) identification. Local autocorrelation images were generated as the pre-treatment for horizontal edge identification, so that the horizontal edge characteristics could be strengthened while the influence of weather conditions could be reduced. Robust background model could be obtained based on exponential forgetting method (EFM), the moving vehicle regions were detected by background subtraction. Stable horizontal edge of vehicle was detected for vehicle tracking, the length of horizontal edge was normalized in image sequence to improve vehicle detection rate. The distance of the barycentric coordinate of the horizontal edges was used to track vehicles in traffic videos. Barycentric coordinate was modified using correction coefficient to ensure the effect of tracking. The vehicle regions were marked using bounding box during vehicle tracking. Traffic videos of various complex conditions (foggy weather, strong sunlight, morning, and evening) were used as test images to verify the effectiveness of the proposed method. Experimental results show that a higher identification rate of moving vehicles is obtained via the proposed method. The proposed novel method can be used to improve the performance of the intelligent transportation systems.

**Keywords:** Vehicle tracking, Local autocorrelation, Horizontal edges, Exponential forgetting method.

## INTRODUCTION

Traffic monitoring and intelligent transportation systems (ITS) have become more important considering the increasing amount of road traffic [1]. Vehicle detection is an important and basic technology in ITS because vehicle tracking allows the enforcement of traffic police with precise information on traffic [2]. Intelligent traffic video analysis is an important part in machine vision and pattern recognition research [3]. Applications including traffic statistics and vehicle identification should be used in traffic systems as quickly as possible. However, several restricting factors exist in their practical application, such as illumination changes, shooting angles, and overlapping vehicles [4]. The existing vision-based systems cannot provide highly accurate information, statistics, and analysis of traffic flow; these systems are limited to the statistical number of vehicles in good environmental conditions [5] or the pattern recognition of specific sub-problems [6, 7], congestion detection, and predictable road transport [8], thereby lacking generality.

Recent research in traffic image analysis has focused on motion vehicle detection and segmentation approaches, as well as vehicle tracking approaches. The study of ITS is a valuable research area to solve the dynamic traffic assignment model. Several researchers

have proposed real-time vehicle identification and tracking methods [9-12]. These methods have higher level recognition capabilities with low-level functionality. The background subtraction method is suitable for detecting foreground objects in a traffic video sequence, where the background is obtained in advance and does not change with the passage of time [13]. These identification methods mostly depend on a Gaussian mixture model or a background subtraction method [14, 15]. Applicable methods of complex situations are needed to deal with changing backgrounds or light conditions [16]. The effects of overlapped vehicles and vehicle shadow in traffic videos are difficult to eliminate for vehicle identification [17, 18]. The vehicle area is extracted using background subtraction [19, 20].

We assume that normal driving vehicles in the traffic lane under various weather conditions are the research objects. The vehicles (for example, cars, buses, trucks) that have obvious horizontal edge feature as tracking objects. In addition, tracking area is limited by traffic lane, the area between the two white traffic lanes is tracking area. The changes of illumination and the impact of the weather are the main factors of restricting the intelligent transportation system applications. The purpose of this paper is to improve the accuracy of vehicle detection and tracking in variety of weather conditions. Local autocorrelation images are generated as the pre-treatment to reduce the influence of weather conditions. Stable horizontal edge of vehicle is detected to achieve vehicle tracking. The proposed novel method achieves high accuracy of the on road driving vehicles detection and tracking , also provides theoretical basis for the construction of intelligent transportation system.

Vehicle tracking is one of the most basal and important technology of vehicle speed detection and forewarning of traffic accident. For the purposes of improving vehicle detection and tracking accurate, normal driving vehicles in the traffic lane are considered tracking object. An improved method for moving vehicle identification and tracking was proposed in this paper, which is based on the horizontal edge (HE) and local autocorrelation (LAC) images. Stable HEs are detected for tracking vehicles in the image sequence [21]. In order to improve vehicle tracking rate, EFM is used to get robust background, position of HE is corrected by using correction coefficient based on reference [21]. The shape of a vehicle is basically symmetrical, and the original images are converted to LAC images. The edge features of the vehicle can be strengthened; thus, the precision of vehicle identification can be improved based on the HE trajectories of the vehicle area. The overlapping vehicles in an image sequence can be separately tracked using HEs in our system.

## 2. VEHICLE IDENTIFICATION ALGORITHM

Stable HE is an important feature of vehicles [22-24]. Thus, we proposed a moving vehicle tracking algorithm based on HE. Candidate HEs are initially detected based on algorithm *A* (enclosed by a solid line, the identification of HE and LAC images is based on the Sobel filter) [25, 26] or algorithm *B* (enclosed by a dotted line, smoothing processing is followed by applying a Sobel filter and finding the local maxima). Stable HE detection is an important part in the algorithm of vehicle tracking. The LAC images and edge detection are utilized to strengthen the edge character in algorithm A before smoothing processing. The Sobel filter and local maxima value are used to detect the HE from a part of the image that shows the edge characteristics. Thus, complementary algorithms *A* and *B* are proposed in our system. Second, the moving object regions can be detected and extracted using the background subtraction method from the input traffic video. The core step of background subtraction is the construction of an adaptively updating background model. The performance of background subtraction algorithms depends on how to construct the background model. Third, the *y*-axis projection counts the frequency of a pixel as a HE on each of the *y*-coordinates to detect stable HEs from the candidate HEs based on the *y*-axis projection and histogram processing. Finally, HEs could be identified in successive frames by tracking and correcting the position of these HEs. Vehicles could be tracked based on stable HEs. The details and process of the algorithm are shown in Fig.1.

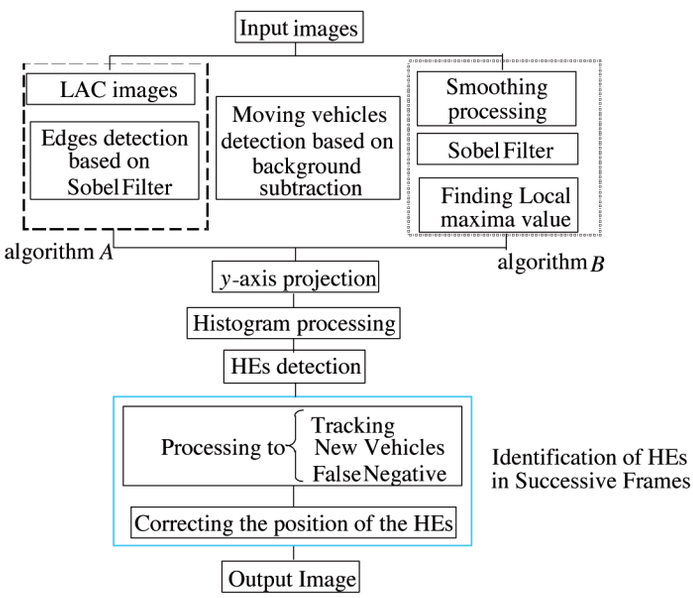


*Fig. 1: Process of the proposed algorithm*

### 2.1. LAC IMAGES

LAC is a local approximation of autocorrelation for improving vehicle features. In digital image processing, the LAC function is used to evaluate image complexity. The calculation of LAC is performed pixel-by-pixel; the operations focus on pixel blocks. The 2D values of LAC are computed as follows:

$$\varphi(x,y,\tau_x,\tau_y)=\frac{\frac{1}{N^2}\sum_{i}^{N}\sum_{j}^{N}I(x+i,y+j)\cdot I(x+i+\tau_x,y+j+\tau_y)}{\frac{1}{N^2}\sum_{i}^{N}\sum_{j}^{N}I(x+i,y+j)^2} \quad (1)$$

Vehicle images have significant HE features. Thus, the LAC coefficients are calculated in the vertical direction. 1D LAC is defined by Equation 2, where the calculation is from $+N/2$ to $-N/2$ for each $N$ value. The vehicle has more horizontal features than vertical features in the traffic images, and the HE feature can be strengthened after using LAC computed in the *y* direction.

$$\varphi(x,y,\tau_y)=\frac{\frac{1}{N}\sum_{i}^{N}I(x,y+i)\cdot I(x,y+i+\tau_y)}{\frac{1}{N+\tau_y}\sum_{j}^{N+\tau_y}I(x,y+i)^2} \quad (2)$$

In this equation, $\varphi(x,y,\tau_y)$ is the object pixel value of LAC, $N$ is the size of the template parameters, and $\tau_y$ is a template of the displacement parameters. Given that $1/(N+\tau_y)$ and $1/N$ introduced the formula of the denominator and molecule, respectively,

the value of $\varphi(x,y,\tau_y)$ was close to 1 even under the small the template size *N*. In addition, the values of the template size *N* and $\tau_y$ displacement value were larger; thus, the smooth effect is more evident. We assume that for the six adjacent pixels, *A*, *B*, *C*, *D*, *E*, and *F*, the value of LAC for $N = 3$ and $\tau_y = 3$ is calculated by Equation 2. In Fig.2, the features in the horizontal direction can be strengthened when the LAC coefficient is used in the vertical direction; this functions as an overview of the calculation with Equation 3. In the present model, *B* is a pixel of interest, whereas *A*, *C*, *D*, *E*, and *F* are adjacent pixels. *A* molecule is the average of the sum of the product of every third pair. Furthermore, the denominator is a root-mean-square of six pixels.

$$\varphi(B,1)=\frac{\frac{1}{3}(A\cdot D+B\cdot E+C\cdot F)}{\frac{1}{6}(A^2+B^2+C^2+D^2+E^2+F^2)} \tag{3}$$


*Fig. 2: Calculation of LAC values (original image).*

An example of the original image calculation of LAC values is shown in Fig.2. The LAC image is shown in Fig.3(a). The relationship between the LAC value and LAC intensity is as follows. The more similar are the adjacent pixels, the stronger is the correlation, with a corresponding greater LAC coefficient. When the value of the coefficient is closer to 1, this value corresponds to LAC with a higher luminance, such as the road surface; thus, the region of gray level change is small. Instead, when the difference between adjacent pixels is larger, the correlation is weaker, which corresponds to a smaller LAC coefficient. When the value of the coefficient is closer to 0, this value corresponds to the LAC brightness of a dark part of the image, such as the edge of the vehicles; thus, the region of gray level change is large.

The processing result of the Sobel filter is shown in Fig.3(b). The Sobel filter detected several horizontal edges. LAC is applied to enhance HE, and Fig.3(c) shows the resulting image. HE detection based on the Sobel filter and the combined LAC and Sobel filter are compared in Fig.3(b) and Fig.3(c). In the comparative analysis of gray value characteristics, the horizontal edges are clearer in Fig.3(c) than in Fig.3(b). Thus, preliminary evidence of the effectiveness of LAC is obtained.

## 2.2. MOVING VEHICLE REGION DETECTION

Moving vehicle regions are detected using background subtraction. The exponential forgetting method (EFM) is used to model traffic video image background. The improved EFM is defined by Equation 4.

$$B_{n+1}(x,y)=\begin{cases}\alpha\cdot B_n(x,y)+(1-\alpha)\cdot I_n(x,y) & if\ M_n(x,y)=0\\ B_n(x,y) & otherwise\end{cases} \tag{4}$$

where $B(x, y)$ is the background image, $I_n(x, y)$ is the current frame image, and $M(x, y)$ is the moving region. $M(x, y)$ is detected by frame subtraction as described by Equation 5.

$$M_n(x,y)=\begin{cases}0 & if\ \ |I_{n+1}(x,y)-I_n(x,y)|<1\ \text{or}\\ & \ \ |I_n(x,y)-I_{n-1}(x,y)|<1\\ 1 & otherwise\end{cases} \tag{5}$$

where $\alpha$ is the weight coefficient, which is calculated by Equation 6. The value of $\alpha$ is from 0 to 1.

$$\alpha=1-\frac{\sum M_n(x,y)}{\sum I_n} \tag{6}$$

Noise is removed using smoothing, which is calculated according to Equation 7.

$$I'(x,y)=\frac{\left\{\sum_{i=-2}^{i=2}\sum_{j=-2}^{j=2}I(x+i,y+i)\right\}+3I(x,y)}{28} \tag{7}$$

Fig. 4(a) shows an example of the original image in fog weather. The moving vehicle regions are detected using background subtraction, and the detected resulting image is shown in Fig.4(b). Therefore, moving vehicles could be accurately detected in the foggy traffic image.

## 2.3. STABLE HORIZONTAL EDGE DETECTION

Our previous research discussed an algorithm of HE detection in detail. Algorithm B will be discussed thoroughly in this paper

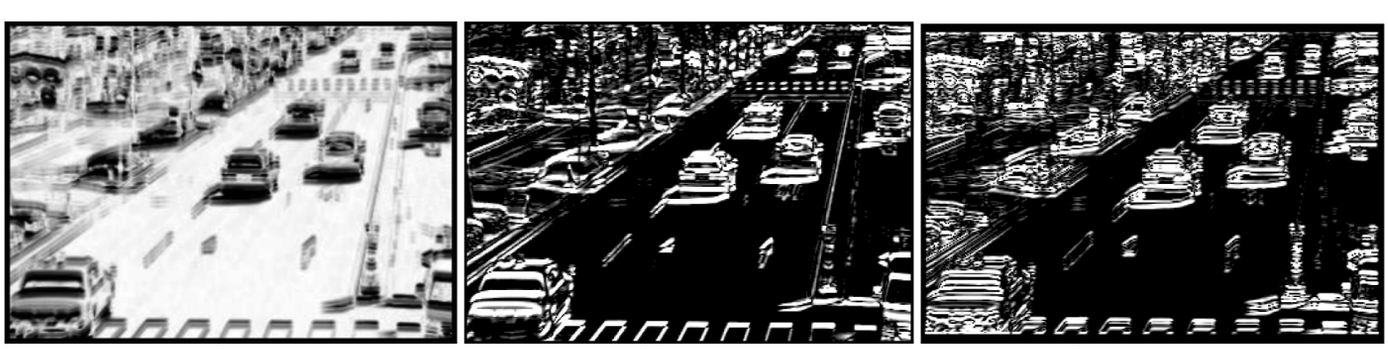


*Fig. 3: Image processing based on LAC and Sobel. (a) LAC image. (b). Sobel filter. (c). LAC and Sobel filter*


*Fig. 4: Background subtraction. (a) Original foggy image. (b) Resulting vehicle regions in foggy weather*

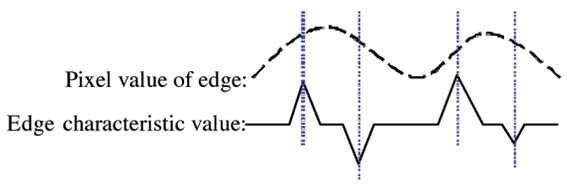


*Fig. 5: Edge characteristics*

to detect more stable HEs in harsh environments. The edge characteristics are shown in Fig.5. The dotted line in the upper region shows the pixel values of edge, whereas the solid line is the edge characteristic value after the differential is obtained. Edge identification could be accomplished by finding the local maxima of the edge characteristic values.

The resulting image of the Sobel filter is shown in Fig.6(a). Based on the maximum value of the entire image, such as when the shadow is included in the vehicle region, erroneous detection is increased. Therefore, threshold processing is used to reduce the false positives. The local maxima of vehicle regions are found by overlapping Fig.4(b) with Fig.6(b). The local maxima of the vehicle regions are shown in Fig.6(c). Candidate horizontal edges in the original image and the vehicle regions are shown in Fig.6(d) and Fig.6(e), respectively.

A moving average filter is calculated as described in Equation 8 to ease the identification of local maxima, thereby smoothing the edge characteristic values before local maximum identification.

$$I''(x,y)=\frac{\left\{\sum_{i=-2}^{i=2} I'(x,y+i)\right\}+I'(x,y)}{6} \tag{8}$$

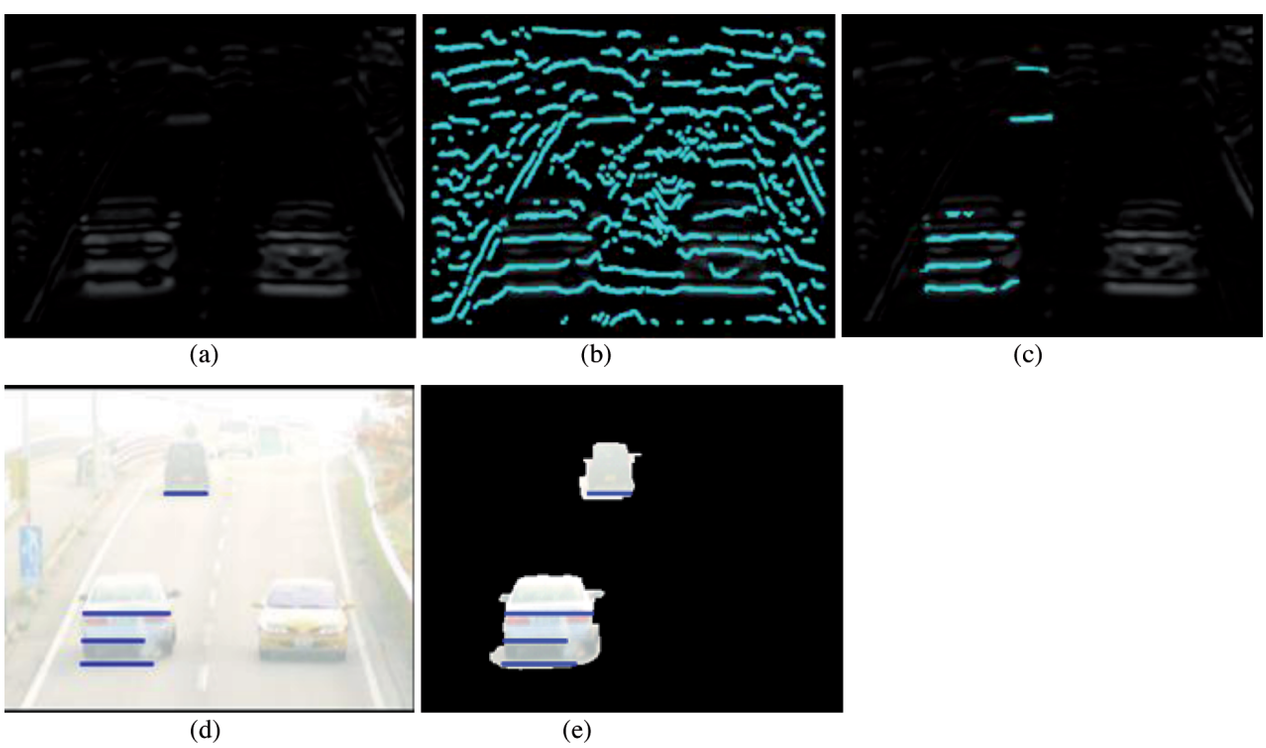


*Fig. 6: Resulting images from processing with algorithm B. (a) Smoothing processing and Soble filter. (b) Local maxima detection. (c) Local maxima of vehicle regions. (d) Candidates for HEs.(e) Candidates for HEs of vehicle regions*

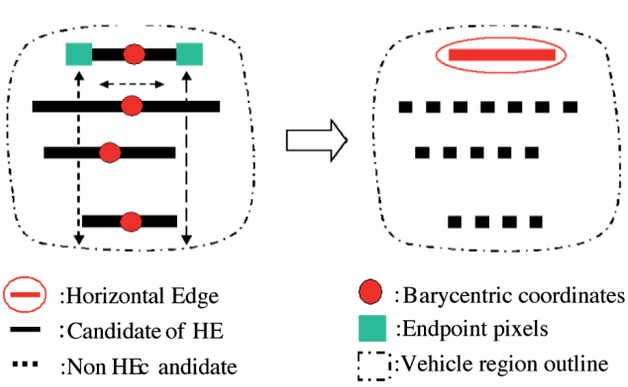


*Fig. 7: Stable HE detection*

The local maxima are found using Equation 9.

$$I''(x,y-1)<I''(x,y)<I''(x,y+1)$$
$$\Rightarrow I''(x,y):\textit{Local mamima} \tag{9}$$

When the vehicle is left at the observation point, the proportion of horizontal edges becomes smaller. The length of HE is normalized with the barycentric coordinate in the *y*-direction. The barycentric coordinate is calculated using Equation 10, where *i* is the label number, $(GX_i, GY_i)$ is the barycentric coordinate of HE, and *p* is the number of pixels.

Vehicle regions with multiple horizontal edges are detected as candidates in Fig.6(c). One vehicle should correspond to only one

HE in the latter part of vehicle tracking. Therefore, only one stable HE should be selected from multiple candidates.

$$\begin{aligned} &f \ \ lable\ number\ of\ \ coordinates\ (x,y)=i \\ &GX_i = GX_i + x \\ &GY_i = GY_i + y \\ &p_i = p_i + i \\ &after\ raster\ scan \\ &GX_i = \frac{GX_i}{p_i} \\ &GY_i = \frac{GY_i}{p_i} \end{aligned} \tag{10}$$

The HE length is normalized by Equation 11, where $L_i$ is the normalized length of HE, $l_i$ is the HE length before normalization, and $R_{GYi}$ is the ratio of barycentric coordinates in the *y*-direction.

$$L_i = l_i \times R_{GY_i} \tag{11}$$

The barycentric coordinates of HE are initially calculated, and endpoint pixels of HE are detected. The left and right endpoints comprise the raster scan region during the subsequent processing. The existence of other barycentric coordinates is investigated. If other barycentric coordinates exist, the HE corresponding to the barycentric coordinate will be eliminated. Fig.7 shows the process of stable HE identification.

The effectiveness of the proposed experimental method under complicated environments (foggy weather, presence of a vehicle shadow, daytime, and evening) is confirmed using the traffic videos as test images. Candidates for horizontal edge identification and stable HE detection of images during the daytime are shown in Fig.8.

(a) (b)

*Fig. 8: HE identification during the daytime. (a) Candidates for HEs detection. (b) Stable HEs detection*

(a) (b)

*Fig. 9: HE identification in foggy weather. (a) Candidates HEs in fog. (b) Stable HEs in fog.*

(a) (b)

*Fig. 10: HE identification in the evening. (a) Candidates HEs in the evening. (b) Stable HEs in the evening*

Fig. 9 and Fig.10 show the images of the candidate HEs and stable HE identification results in foggy weather and the evening, respectively.

The results of stable HE detection under different conditions are shown in Figs. 8, 9, and 10. Stable HEs are marked in two colors: blue and red. The blue and red HEs are detected by algorithms *B* and *A*, respectively.

The experimental results showed that the proposed method is effective in various conditions, whereas algorithm *B* can compensate for the lack of an algorithm. A robust HE identification method is obtained by combining algorithms *B* and *A*. Table 1 shows the results of tracking labeled HE in a moving image.

Table 1. HE tracking of the moving images.

| Tracking label | Ground truth (number) | Tracking result (number) | False positive (number) | False negative (number) | Rate (%) |
|---|---|---|---|---|---|
| 1 | 90 | 90 | 0 | 0 | 100 |
| 2 | 103 | 103 | 0 | 0 | 100 |
| 3 | 108 | 105 | 0 | 3 | 94.6 |
| 4 | 125 | 125 | 0 | 0 | 100 |
| 5 | 120 | 120 | 0 | 0 | 100 |
| 6 | 126 | 125 | 1 | 0 | 98.4 |
| 7 | 125 | 125 | 0 | 0 | 100 |
| 8 | 121 | 121 | 0 | 0 | 100 |
| 9 | 119 | 114 | 0 | 5 | 91.9 |
| 10 | 42 | 42 | 0 | 0 | 100 |
| Ave | / | / | / | / | 98.5 |

## 3. VEHICLE IDENTIFICATION AND TRACKING BASED ON STABLE HORIZONTAL EDGE

### 3.1. VEHICLE IDENTIFICATION

In this experimental system, the calculation of each HE barycentric coordinate is based on the *y*-coordinates. HE tracking should be used in consecutive corresponding relationships between consecutive windows to apply the center of gravity of HE.

Moving vehicles are tracked by using the HE barycentric coordinates in the vehicle identification system. *I(i)* is computed by Equation 12; this value is the minimum distance between barycentric coordinates in the *y*-coordinate axis. In this equation, $L_i(j)$ is the distance between two frames, $i(t-1)$ and $j(t)$ are the numbers of frames.

$$\begin{aligned} &I(i) = \arg\min_j L_i(j) \\ &L_i(j) = \left| y_{j(t)} - y_{i(t-1)} \right| \end{aligned} \tag{12}$$

A vehicle will be detected as a new vehicle when it goes through the tracking window, and the HE of the new vehicle can be tracked for at least five consecutive frames. Vehicles move in the adjacent area, such that the tracking window is near the new target being detected. If HE is detected in 5 consecutive frames, the tracking label is labeled to an initial vehicle. Fig.11 is an overview of the process of new object identification.

We initially detected the HE that is closest to the barycentric coordinate of the tracking window. HE identification is based on

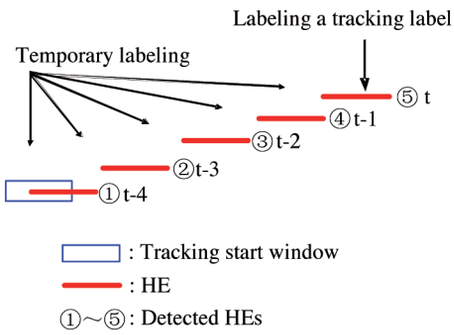


*Fig. 11: Overview of new vehicle identification*

the distance between the barycentric coordinate of the tracking window and barycentric coordinate of the marked HE. A provisional label is attached to the HE that has been detected. In the next frame, if the HE can be tracked for at least five following consecutive frames, the said HE will be detected as a new vehicle HE and the corresponding tracking labels are attached.

### 3.2. VEHICLE TRACKING

The correspondence of successive HE tracking is indispensible between two contiguous frames. The *y*-coordinates of horizontal edges are used to compute the barycentric coordinates of HE. The distance of the barycentric coordinates of horizontal edges is computed using Equation 13.

$$d_{Ti}(i)=\sqrt{(GX_{Ti}-GX_i)^2+(GY_{Ti}-GY_i)^2} \tag{13}$$

$GX_{Ti}$ and $GY_{Ti}$ are barycentric coordinates of the tracked HE. The minimum of $d_{Ti}(i)$ is computed by Equation 14.

$$T(Ti)=\arg\min_{Ti} d_{Ti}(i) \tag{14}$$

Where $T_i$ is the label number of the tracked HE. A schematic of HE tracking is shown in Fig.12.

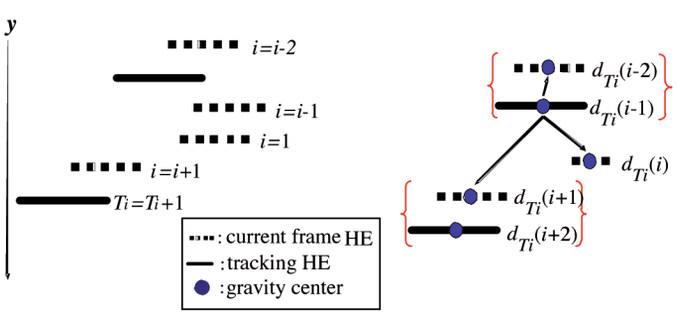


*Fig. 12: Overview of HE tracking*

In addition, the tracked HE exits the tracking range. In the current frame, when the tracked HE exceeds the *y*-coordinate of the end position, tracking is exited. Afterward, the frame over the succeeding frame is assumed to unable to keep tracked HE.

The frame rate ranges distinctly from 20 fps to 30 fps. The displacement of a moving vehicle within a frame is small; thereby, the distance between HEs is also small. However, the position of coordinate swings between frames; thus, correction is needed to ensure that the position of each barycentric coordinate corresponds to the actual movement of the vehicle. Fig.13 shows the method for correcting the HE position. The correction coefficient is calculated from the traveled distance of each barycentric coordinate.

$SP(i) = FP(i-1)$
$SP$ = Starting Point
$FP$ = Finishing Point
$i$ = Group number per frames

$y_i, x_i$ ( Travel distance / n frames )

$Y_i, X_i$ ( average travel distance / frame )

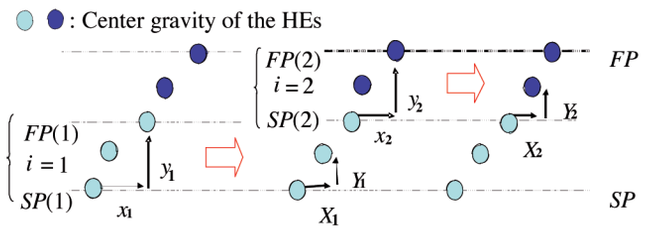


*Fig. 13: Overview of correcting the HE position*

A comparison of the barycentric coordinates before and after correction is shown in Fig.14. The horizontal axis and vertical axis of Fig.14 are pixel location of barycentric coordinates in *x* direction and *y* direction respectively. Fig.14 shows the offset of barycentric coordinates. The corrected barycentric coordinates are more stable and precise than those before correction.

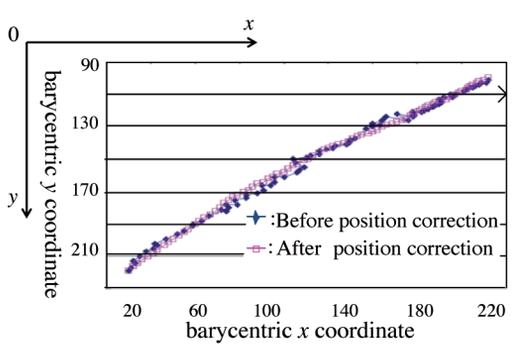


*Fig. 14: Comparison of barycentric coordinates before and after correction*

The bounding box is used to mark the vehicle region during vehicle tracking. The length of the top side of the bounding box is calculated based on Equation 15, where $SPL_{Ti}$ is the length of HE in the starting point, and $BL_{(Ti,m)}$ is the length of the top side of the bounding box.

$$BL_{(Ti,m)}=SPL_{Ti}\times\frac{R_{oy_{(Ti,m)}}}{R_{oy_{(Ti,m)}}} \tag{15}$$

From the position of the barycentric coordinate to the left and right sides, a line segment is drawn, and the length of this line is $BL_{(Ti,m)}$. A generated example of the bounding box is shown in Fig.15. The red point is the barycentric coordinate of the HE. The $BL_{(Ti,m)}$ value is the length of the straight line that is drawn from

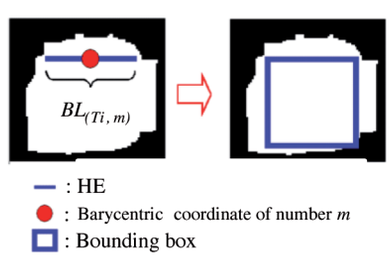


*Fig. 15: Generation of the bounding box*

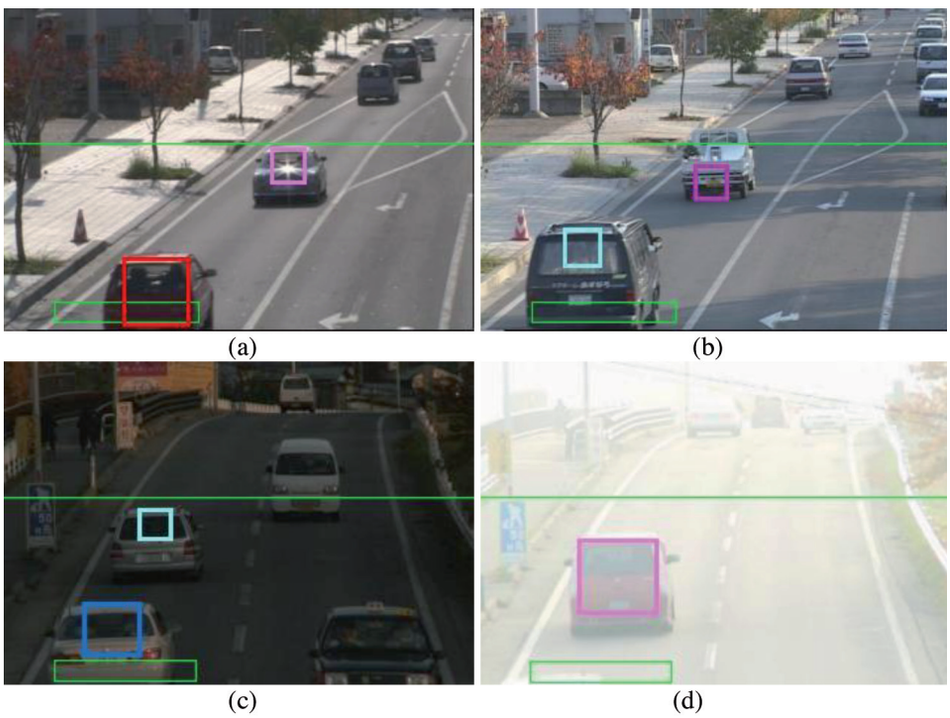


*Fig. 16: Tracking results. (a) Tracking results in the morning. (b) Tracking results during daytime. (c) Tracking results in the evening.(d) Tracking results in fog*

the left and right endpoints of the HE to the direction of the vehicle region. Finally, the square bounding box region is generated.

The Sobel filter method and the proposed HE method were used to track vehicles at different times of the day (morning, daytime, and nightfall) to verify the validity of the proposed method. The frames processed by the Sobel filter were labeled "1", whereas those formed after processing with the proposed method were labeled "2". A comparison of tracking results is shown in Table 2. The proposed method was more stable for more values than the Sobel filter method. For instance, the luminance values of the region of interest were smaller with HE, such that a strong horizontal edge could be detected.

## 4. EXPERIMENTAL RESULTS

In order to obtain comparable results, the same traffic videos database as [21] are used. For the experimental vehicle tracking, traffic videos under various conditions, such as morning, daytime, evening, and foggy weather, are used as test images. The experimental results of vehicle tracking in the morning and daytime are shown in Fig.16(a) and Fig.16(b), respectively. Fig.16(c) and Fig.16(d) show results of tracking images in the evening and fog weather. Results show that each vehicle can be detected even with the existence of a vehicle shadow. Under normal lighting, the floor of the vehicle and the background are apparently different; thus, the moving vehicles can be successfully detected and tracked based on the HE method. In the evening and fog weather, the lighting conditions are poor, such as in Fig.16(c) and Fig.16(d), respectively. Thus, the vehicle is similar to the background, but the HE method can still identify and track moving vehicles.

Table 2: Comparison of tracking results

| Time conditions | Frame (number) | Tracking method | Tracked result (number) | Lost result (number) | Tracking rate (%) |
|---|---|---|---|---|---|
| Morning | 561 | 1 | 561 | 0 | |
| | | 2 | 549 | 14 | 97.8 |
| Daytime 1 | 842 | 1 | 834 | 8 | 99.0 |
| | | 2 | 833 | 9 | 98.9 |
| Daytime 2 | 896 | 1 | 882 | 14 | 98.4 |
| | | 2 | 876 | 20 | 97.7 |
| Daytime 3 | 376 | 1 | 375 | 1 | 99.7 |
| | | 2 | 365 | 9 | 97.1 |
| Daytime 4 | 1125 | 1 | 1111 | 14 | 98.8 |
| | | 2 | 1096 | 29 | 97.4 |
| Nightfall | 676 | 1 | 674 | 2 | 99.7 |
| | | 2 | 669 | 7 | 98.9 |

Table 3 shows the vehicle tracking results in the four studied conditions. The average identification rate was 91.1%. Although the identification rates did not reach 90% in daytime and foggy weather, a higher identification rate was achieved based on the HE method. Fig.17 shows Comparison of vehicle tracking results under various weather conditions. The horizontal axis and vertical axis of Fig.17 are identification rates and weather conditions respectively. According to experimental results, the shadow of the vehicle affected the identification rates, especially during the daytime. We intend to focus on vehicle shadow identification in our future work. Although not all vehicles could be identified and tracked, a

Table 3: Vehicle tracking results.

| Weather conditions | Vehicle (number) | Identification result (number) | Identification rate (%) |
|---|---|---|---|
| Morning | 15 | 14 | 93.3 |
| Daytime | 16 | 14 | 87.5 |
| Evening | 18 | 17 | 94.4 |
| Foggy weather | 19 | 17 | 89.4 |
| Total/Ave | 68 | 62 | 91.1 |

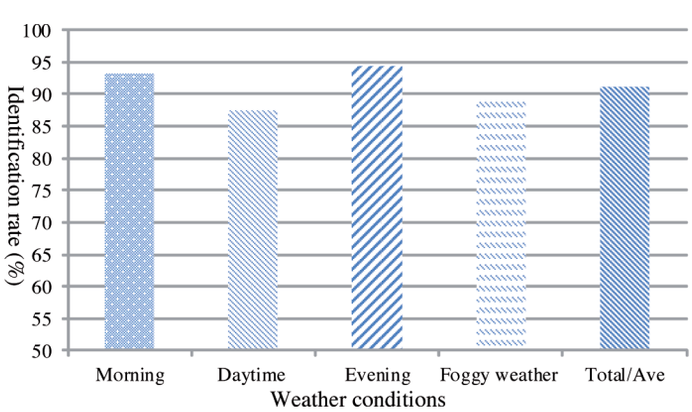


*Fig. 17: Comparison of vehicle tracking results under various weather conditions*

high recognition rate could be achieved with LAC and HE identification in complex conditions.

## 5. CONCLUSION

This paper proposed a novel method for moving vehicle detection and tracking based on HE identification and LAC images. The horizontal features were strengthened, and the influence of weather condition was reduced by the use of LAC images. The effectiveness of our tracking algorithm, which used HEs of each vehicle, was demonstrated in the experiment. Results show that vehicle measurement based on traffic video processing is considerably feasible in traffic control applications. The proposed method should be verified for more traffic images in other conditions in our future work. The identification rate should also be improved by removing the vehicle shadow. After addressing this issue, our algorithm will determine other applications, such as the monitoring of vehicle speed, the distance between two vehicles, and the direction of individual running vehicles.

## BIBLIOGRAPHY

[1] Leibe B, Schindler K, Cornelis N, et al. "Coupled object detection and tracking from static cameras and moving vehicles". *IEEE Transactions on Pattern Analysis and Machine Intelligence*. October 2008. Vol. 30-10. p.1683–1698. DOI: http://dx.doi.org/10.1109/TPAMI.2008.170

[2] Wang Y. "Joint random field model for all-weather moving vehicle detection". *IEEE Transactions on Image Processing*. September 2010. Vol. 19-9. p.2491-2501. DOI: http://dx.doi.org/10.1109/TIP.2010.2048970

[3] Sakai Y, Miyoshi M, Tan J K, et al. "Extracting mobile objects by sequential background detection on a video". *Artificial life and Robotics*. December 2008. Vol. 13-1. p.302-305. DOI: http://dx.doi.org/10.1007/s10015-008-0537-1

[4] Palubinskas G, Kurz F, Reinartz P. "Model based traffic congestion detection in optical remote sensing imagery". *European Transport Research Review*. June 2010. Vol. 2-2. p.85-92. DOI: http://dx.doi.org/10.1007/s12544-010-0028-z

[5] Zeng H, Wang X, Cai C, et al. "Fast multiview video coding using adaptive prediction structure and hierarchical mode decision". *IEEE Transactions on Circuits and Systems for Video Technology*. September 2014. Vol. 24-9. p.1566-1578. DOI: http://dx.doi.org/10.1109/TCSVT.2014.2310143

[6] Li L, Huang W, Gu I.Y. H, et al. "Statistical modeling of complex backgrounds for foreground object detection". *IEEE Transactions on Image Processing*. November 2004. Vol. 13-11. p.1457-1472. DOI: http://dx.doi.org/10.1109/TIP.2004.836169

[7] Xu B, Xie S, Li Z. "Research of Anti-Noise Image Salient Region Extraction Method". *Journal of Engineering Science and Technology Review*. January 2014. Vol. 7-1. p.143-147.

[8] Yue H, Cai K, Luo B, et al. "Denoising and Segmentation of Digital Feather Image Using Mean Shift Algorithm". *Journal of Digital Information Management*. February 2015. Vol. 13-1. p.25-30.

[9] Nawaz T, Poiesi F, Cavallaro A. "Measures of effective video tracking". *IEEE Transactions on Image Processing*. November 2013. Vol. 23-1. p.376-388. DOI: http://dx.doi.org/10.1109/TIP.2013.2288578

[10] Betke M, Haritaoglu E, Davis L. S. "Real-time multiple vehicle detection and tracking from a moving vehicle". *Machine Vision and Applications*. August 2000. Vol. 12-2. p.69-83. DOI: http://dx.doi.org/10.1007/s001380050126

[11] Sivaraman S, Trivedi M. M. "Active learning for on-road vehicle detection: a comparative study". *Machine vision and applications*. April 2014. Vol. 25-3. p.599-611. DOI: http://dx.doi.org/10.1007/s00138-011-0388-y

[12] Hsieh J. W, Chen L. C, Chen D. Y. "Symmetrical SURF and its applications to vehicle detection and vehicle make and model recognition". *IEEE Transactions on Intelligent Transportation Systems*. January 2014. Vol. 15-1. p.6-20. DOI: http://dx.doi.org/10.1109/TITS.2013.2294646

[13] Stauffer C, Grimson W. E. L. "Learning patterns of activity using real-time tracking". *IEEE Transactions on Pattern Analysis and Machine Intelligence*. August 2000. Vol. 22-8. p.747-757. DOI: http://dx.doi.org/10.1109/34.868677

[14] Akula A, Khanna N, Ghosh R, et al. "Adaptive contour-based statistical background subtraction method for moving target detection in infrared video sequences". *Infrared Physics and Technology*. March 2014. Vol. 63. p.103-109. DOI: http://dx.doi.org/10.1016/j.infrared.2013.12.012

[15] Wan Y, Huang Y, Buckles B. "Camera calibration and vehicle tracking: Highway traffic video analytics". *Transportation Research Part C Emerging Technologies*. July 2014. Vol. 44. p.202-213. DOI: http://dx.doi.org/10.1016/j.trc.2014.02.018

[16] Kervrann C, Boulanger J. "Optimal spatial adaptation for patch-based image denoising". *IEEE Transactions on Image Processing*. October 2006. Vol. 15-10. p.2866-2878. DOI: http://dx.doi.org/10.1109/TIP.2006.877529

[17] Ramirez A, Ohn-Bar E, Trivedi M. "Integrating motion and appearance for overtaking vehicle detection". *2014 IEEE Intelligent Vehicles Symposium Proceedings*. June 2014. p.96-101. DOI: http://dx.doi.org/10.1109/IVS.2014.6856598

[18] Jazayeri A, Cai H, Zheng J. Y, et al. "Vehicle detection and tracking in car video based on motion model". *IEEE Transactions on Intelligent Transportation Systems*. March 2011. Vol. 12-2. p.583-595. DOI: http://dx.doi.org/10.1109/TITS.2011.2113340

[19] Teoh S. S, Braunl T. "Symmetry-based monocular vehicle detection system". *Machine Vision and Applications*. September 2012. Vol. 23-5. p.831-842. DOI: http://dx.doi.org/10.1007/s00138-011-0355-7

[20] Chan Y. M, Huang S. S, Fu L. C, et al. "Vehicle detection and tracking under various lighting conditions using a particle Filter". *IET Intelligent Transport Systems*. March 2012. Vol. 6-1. p.1-8. DOI: http://dx.doi.org/10.1049/iet-its.2011.0019

[21] Zhu H, Fan H, Guo S. "Moving Vehicle Detection and Tracking in Traffic Images Based on Horizontal Edges". *TELKOMNIKA Indonesian Journal of Electrical Engineering*. November 2013. Vol. 11-11. p.6477-6483. DOI: http://dx.doi.org/10.11591/telkomnika.v11i11.3485

[22] Zhang B, Gu Y. "License plate location algorithm based on multiresolution edge detection". *Lecture Notes in Electrical Engineering*. April 2013. Vol. 163. p.2103-2110. DOI: http://dx.doi.org/10.1007/978-1-4614-3872-4_268

[23] Wu B. F, Kao C. C, Jen C. L, et al. "A Relative-Discriminative-Histogram-of-Oriented-Gradients-Based Particle Filter Approach to Vehicle Occlusion Handling and Tracking". *IEEE Transactions on Industrial Electronics*. October 2013. Vol. 61-8. p.4228-4237. DOI: http://dx.doi.org/10.1109/TIE.2013.2284131

[24] Wu B. F, Juang J. H. "Adaptive vehicle detector approach for complex environments". *IEEE Transactions on Intelligent Transportation Systems*. February 2012. Vol. 13-2. p.817-827. DOI: http://dx.doi.org/10.1109/TITS.2011.2181366

[25] Kuo Y. C, Pai N. S, Li Y. F. "Vision-based vehicle detection for a driver assistance system". *Computers and Mathematics with Applications*. April 2011. Vol. 61-8. p.2096-2100. DOI: http://dx.doi.org/10.1016/j.camwa.2010.08.081

[26] Guo C. Z, Yamabe T, Mita S. "Drivable Road Boundary Detection for Intelligent Vehicles based on Stereovision with Plane-induced Homography". *Acta Automatica Sinica*. April 2013. Vol. 39-4. p.371-380. DOI: http://dx.doi.org/10.1016/S1874-1029(13)60036-1

## APPRECIATION

The study was funded by the Natural Science Fund of Jiangsu Province under Grant No.BK20130235), Natural Science Fund of Changzhou under Grant No.CJ20140049, China National Natural Science Fund of China under Grant No.61302124 and No.61472166, Natural Science Foundation of the Higher Education Institutions of Jiangsu Province under Grant No. 13KJB520006, and Program of six talent tops of Jiangsu Province under Grant No.DZXX-031, Scientific Research Foundation of Jiangsu University of Technology under Grant No. KYY14020.

## SUPPLEMENTARY MATERIAL

We have done publicly available our experiments data in the cloud disk (http://yunpan.cn/cLduueFWAeSHT), if anyone needs the experiments data, please contact the corresponding author (email: fanhonghui@jsut.edu.cn ), we will provide the extracted code.